Liu *et al. Chem. Biol. Technol. Agric.* (2023) 10:122
https://doi.org/10.1186/s40538-023-00495-4

Chemical and Biological Technologies in Agriculture

RESEARCH

Open Access

# Structural characterization, physicochemical property, and antioxidant activity of polysaccharide components from *Eucommia ulmoides* leaves

Mengpei Liu[1†], Yan Wang[2†], Rong Wang[1], Qingxin Du[2] and Lu Wang[2*]

## Abstract

**Background** *Eucommia ulmoides* (*E. ulmoides*) leaves are identified as a new resource of medicine and food homology. In this study, the structural characterization, physicochemical properties, and antioxidant activity of *E. ulmoides* polysaccharides (EUP) were studied.

**Results** Three components with different molecular weights of $1.51\times10^5$ Da ($EUP_1$), $3.05\times10^4$ Da ($EUP_2$) and $1.17\times10^5$ Da ($EUP_3$) were purified from *E. ulmoides* leaves. They were composed of *L-rhamnose* (*Rha*), *D-arabinose* (*Ara*), *D-mannose* (*Man*), D-*glucose* (*Glu*) and *D-galactose* (*Gal*), while $EUP_2$ also contained small amounts of *D-xylose* (*Xyl*). Three components all had typical polysaccharides absorption peaks, which may be polysaccharides with β configuration of pyranose structure, and amorphous structure of acid polysaccharides with good thermal stability below 270 ℃. However, the molecular weight, monosaccharide composition and apparent morphology of the three components were different, resulting in a stronger scavenging ability of $EUP_2$ and $EUP_3$ against DPPH and OH free radicals.

**Conclusion** The results will provide a theoretical reference for developing EUP-related foods and drugs.

**Keywords** *Eucommia ulmoides*, Molecular weight, Thermal stability, Electron spin resonance, Natural antioxidant

†Mengpei Liu and Yan Wang have contributed equally to this work.

*Correspondence:
Lu Wang
Luwang@caf.ac.cn
Full list of author information is available at the end of the article

**Graphical Abstract**

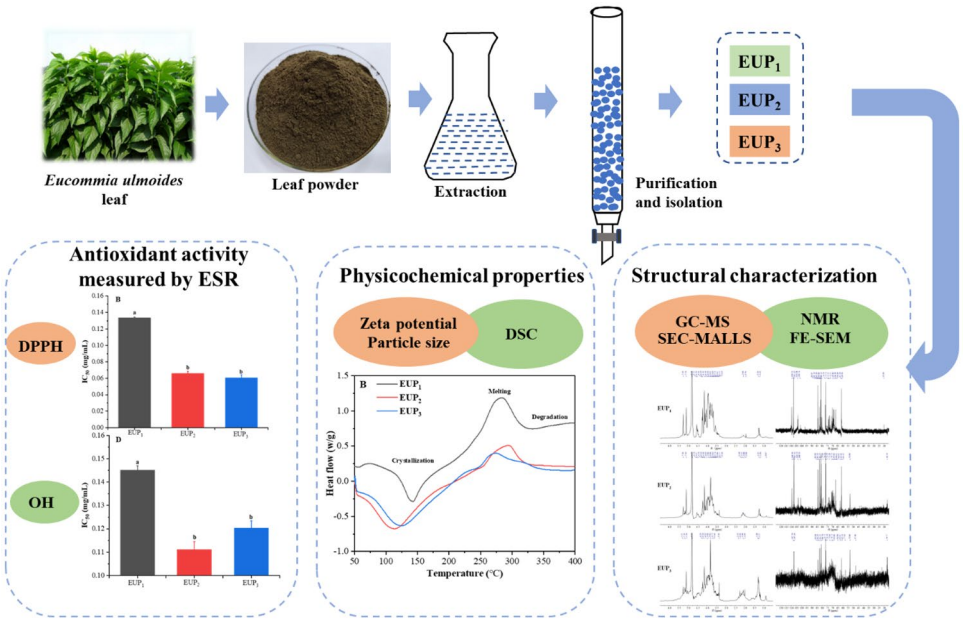


## Introduction

*Eucommia ulmoides* is a rare traditional Chinese medicine. The earliest understanding and utilization of *E. ulmoides* can be traced back to Sheng Nong's herbal classic, which was published 2000 years ago [1]. Traditionally, *E. ulmoides* bark is mainly used because it has various pharmacological effects such as lowering blood pressure, increasing body immunity, antibacterial, antiviral, and so on [2]. Recently, the flowers, seeds and leaves of *E. ulmoide*s have also been included in the homology list of medicine and food in the Chinese National Health Commission. Studies have shown that *E. ulmoides* leaves contain similar active ingredients as bark, which also has good medicinal and edible value. At present, more than 100 active substances have been isolated from *E. ulmoides* leaves, mainly including polysaccharides, flavonoids, chlorogenic acid, geniposidic acid, etc. [3].

Natural polysaccharides obtained from plants have been proven to have high activity, low toxicity, good biocompatibility and biodegradability [4]. In recent years, numerous plant polysaccharides have been isolated and extracted from plants, particularly medicinal and edible homologous plant resources, such as *Lycium barbarum*, *Mentha haplocalyx, Ziziphus jujuba* [5–8]. *Eucommia ulmoides* leaves are a new medicinal and food homologous plant resources. Studies have found that polysaccharides isolated from *E. ulmoides* leaves possess an important antioxidant capacity with effective scavenging activities on radicals [9]. Our previous study also confirmed this conclusion [10]. Moreover, *E. ulmoides* polysaccharides (EUP) have been proved to be beneficial in regulating the immune behavior of macrophages and promoting the enhancement of immune capacity [11]. More importantly, EUP also has anti-inflammatory effects and bone immunomodulatory function [12, 13].

Although EUP has significant antioxidant, anti-inflammatory, immunity enhancement and bone strengthening effects, few studies have focused on the structural characteristics and activity differences of EUP components. In this research, polysaccharide components from *E. ulmoides* leaves were prepared and purified by microwave-assisted extraction combined anion exchange column method, and their molecular weight, monosaccharide composition and structure were studied by size-exclusion chromatography (SEC)-multi-angle laser light scattering (MALLS) gel chromatography, gas chromatography-mass spectrometry (GC–MS), Fourier transform infrared spectrometer (FT-IR), X-ray diffraction (XRD), nuclear magnetic resonance (NMR) and field emission scanning electron microscopy (FE-SEM). The physicochemical property of EUP components were analyzed by zeta potential, particle size and differential scanning calorimetry (DSC), and the antioxidant activity of EUP components was researched by electron spin resonance (ESR). The results will provide a theoretical reference for developing EUP-related foods and drugs.

## Materials and methods

### Materials

*E. ulmoides* (Huazhong 2) leaves were collected from the *E. ulmoides* Research Base in Yuanyang County, Xinxiang City, Chinese Academy of Forestry in September 2021. After picking, the samples were dried at 50 ℃ in the oven until constant weight, crushed and sieved to obtain 250 μm powder, and stored for analysis.

### Crude polysaccharides preparation

The polysaccharides of *E. ulmoides* leaves were extracted according to the previous method with minor modifications [14]. The *E. ulmoides* leaves powder and distilled water were mixed at a ratio of 1:30 (g: mL), and heated in a water bath at 40 ℃ for 2 h. Then it was put in a microwave oven (M1-L213, Midea Group Co., Ltd, Guangdong province, China), and extracted at 230 W for 1.5 min. The extract was centrifuged at 4000*g*×10 min, and concentrated. Anhydrous ethanol was added to reach 80% of the total concentration of the solution, and reacted at 4 ℃ for 24 h. After centrifugation, the precipitate was freeze-dried to obtain crude polysaccharides from *E. ulmoides* leaves. The formula for calculating the extraction rate of crude polysaccharides was shown in Eq. (1):

$$\text{Extraction rate}\,(\%) = \frac{m}{M} \times 100, \tag{1}$$

m: The weight of crude EUP. M: The weight of pretreated sample.

### Crude polysaccharides purification

The method of crude polysaccharides purification was based on a previous work with some modifications [15]. The crude polysaccharides solution (200 mg/mL, 20 mL) was added to macroporous resin AB-8 column (1.6 cm×30 cm), eluted with distilled water and concentrated. The concentrated solution was put into a dialysis bag for 24 h (retained molecular weight = 3500 Da), and EUP was obtained by freeze-dried.

The EUP was dissolved in distilled water (10 mg/mL, 20 mL) and then added to a DEAE-52 column (1.6 cm×40 cm) through 0.45 μm filter membrane. Then, 0.1 mol/mL, 0.2 mol/mL, and 0.3 mol/mL NaCl solutions were successively eluted at a flow rate of 1 mL/min. An automatic collector (DBS-100, Shanghai Huxi Analytical Instrument Co., Ltd., Shanghai, China) was used to collect, and phenol–sulfuric acid method was used to monitor at 490 nm. According to the elution curve, three components were obtained, collected, concentrated, dialysis, freeze-dried, and named $EUP_1$, $EUP_2$ and $EUP_3$, respectively.

### Structural characterization of polysaccharides

#### *Molecular weight distribution*

The detection method of molecular weight distribution of $EUP_1$, $EUP_2$ and $EUP_3$ was assayed as described previous study with minor changes [16]. The $EUP_1$, $EUP_2$ and $EUP_3$ samples were prepared into 1 mg/mL solution and filtered through 0.45 μm membrane. A mixture of 50 mmol/L $NaNO_3$ and 0.02% $NaN_3$ was used as the mobile phase. The molecular weight of polysaccharides was determined by SEC–MALLS gel chromatography system (Wyatt Technology Co., California, USA) with an injection volume of 1 μL and a flow rate of 0.45 mL/min.

#### *Monosaccharide composition*

The monosaccharide composition of $EUP_1$, $EUP_2$ and $EUP_3$ was based on the procedure of a previous study with slight modifications [17]. 3 mL 2 mol/L trifluoroacetic acid was added to 3 mg $EUP_1$, $EUP_2$ and $EUP_3$ samples, respectively, reacted at 120 ℃ for 4 h, evaporated, and washed with methanol 5 times. The treated samples were added to 10 mg hydroxylamine hydrochloride and 0.5 mL pyridine and reacted at 90 ℃ for 30 min, and cooled. Then, 0.5 mL acetic anhydride was added and reacted at 90 ℃ for 30 min, evaporated, and dried. The dried samples were dissolved in methanol and reduced to 5 mL, then filtered through 0.22 μm membrane for GC–MS (Agilent Technologies 7890B, Palo Alto, California, USA) equipped with an HP-5 capillary column (60 m×0.25 mm×0.25 μm). Standard monosaccharides: *L-rhamnose* (*Rha*), *D-arabinose* (*Ara*), *D-mannose* (*Man*), *D-glucose* (*Glu*), *D-galactose* (*Gal*) and *D-xylose* (*Xyl*) were derived by the same method to determine the retention time and standard curve.

The temperature of a detector was 250 ℃ during operation and mobile phase was helium. The scheme for temperature control of the column was as follows: initial temperature was 100 ℃, rising to 200 ℃ at 5 ℃/min for 1 min, and then rising to 250 ℃ at 10 ℃/min for 5 min. The carrier gas flow rate was 1.0 mL/min, and 1 μL was injected regardless of the flow rate. The conditions of mass spectrometry were interface temperature of 280 ℃, quadrupole temperature of 150 ℃, electron bombardment energy of 70 eV, solvent extension time of 5 min and full scanning range m/z of 50–800.

#### *FT-IR spectrum*

The infrared spectroscopy analysis of $EUP_1$, $EUP_2$, and $EUP_3$ was performed using the method of the previous study with some changes [18]. The samples (3 mg) and KBr solid powder (300 mg) were mixed and extruded. A FT-IR spectrometer (Vertex 70, Bruker Instruments, Billerica, Germany) was used to analyze the characteristic

spectra of $EUP_1$, $EUP_2$ and $EUP_3$, with a scanning wave number range of 4000–400 $cm^{-1}$, resolution of 4 $cm^{-1}$, and cumulative scanning of 64 times.

#### *Crystal structure*

Based on the reported method [19], the crystal structure of the polysaccharides was determined using a XRD powder diffratometer (D8 Advance, Bruker Instruments, Billerica, Germany) with a diffraction Angle (2Θ) of 10° to 80°, step size of 0.05° (2Θ) and time of 1 s/step.

#### *NMR analysis*

NMR spectra of $EUP_1$, $EUP_2$, and $EUP_3$ were determined using an AVANCE III spectrometer (Bruck, Germany). Each sample (10 mg) was dissolved in 0.55 mL of $D_2O$. The fully dissolved samples were then transferred to NMR tubes, and $^1H$ NMR and $^{13}C$ NMR spectra were analyzed by NMR at room temperature.

#### *FE-SEM*

The surface microstructures of $EUP_1$, $EUP_2$, and $EUP_3$ were observed by FE-SEM (SU8100, Hitachi, Tokyo, Japan). Polysaccharides samples were sprayed with gold, and the images of sample powders at 10 K× multiples were observed under a high vacuum at 3 kV acceleration voltage.

### Physicochemical property of polysaccharides

#### *Zeta potential and particle size*

The zeta potential and mean particle size of each polysaccharides solution (1 mg/mL) were measured at 25 ℃ using a nano-particle size potentiometer (Zetasizer Nano ZS90, Malvern Instruments, Malvern, UK).

#### *Thermal stability*

The thermal stability of the polysaccharides was analyzed by DSC (DSCQ20, TA Instruments, New Castle De, USA) [20]. 3 mg polysaccharides samples were placed into an aluminum crucible for analysis at a temperature range of 50–400 ℃, heating rate of 10 ℃/min, and nitrogen flow rate of 1 s/step.

### Antioxidant activity

#### *DPPH radical scavenging activity*

According to the reported method [21], DPPH radical scavenging ability of polysaccharides was determined by ESR (E-scan, Bruker Instruments, Billerica, Germany). The 50 μL polysaccharides solutions were evenly mixed with 0.2 mmol/L 50 μL DPPH solution, and dark reaction was performed at 25 ℃ for 2 h. The mixtures were then moved into a quartz capillary and placed into a resonant cavity for measurement. The ESR measurement conditions were frequency of 9.792069 GHZ, power of 5.0 mW, central magnetic field of 3487 Gauss modulation amplitude of 2.27 Gauss, modulation frequency of 86.00 KHZs, sweep time of 83.88 s. After the test, the DPPH radical scavenging ability was calculated according to the quadratic integral value, and the integral region was 3450–3525 Gauss. Methanol solution was used instead of the polysaccharides solution as the blank group. DPPH free radical clearance was calculated as follows Eq. (2):

$$\mathrm{RSA}(\%) = \frac{(A_0 - A)}{A_0} \times 100, \tag{2}$$

$A_0$: Quadratic integral value of the characteristic peaks of the blank group.

A: Quadratic integral value of the characteristic peaks of the sample group.

#### *OH radical scavenging activity*

The OH radical scavenging of $EUP_1$, $EUP_2$ and $EUP_3$ was based on the procedure of a previous study with slight modifications [22]. Since OH radicals exist for a short time in aqueous solution at room temperature and cannot be detected by ESR, DMPO (5,5-dimethyl-1-pyrroline N-oxide) was added as a hydroxyl radical capture agent in the reaction system to combine with the free radicals to form stable free radical adduct. 50 μL polysaccharides solution, 50 μL DMPO, 40 mmol/L, 50 μL $FeSO_4$ solution and 40 mmol/L, 200 μL $H_2O_2$ were mixed in turn, and the dark reaction lasted for 10 min. The experimental conditions of ESR were the same as those of the DPPH radical, and only the scanning time was changed to 20.97 s. The calculation formula of OH radical scavenging was shown in Eq. (3):

$$\mathrm{RSA}(\%) = \frac{(B_0 - B)}{B_0} \times 100, \tag{3}$$

$B_0$: Quadratic integral value of the characteristic peaks of the blank group.

B: Quadratic integral value of the characteristic peaks of the sample group.

### Statistical analysis

All determinations were performed in triplicate and the corresponding data were presented as the mean of three determinations ± SE (Standard error). Data analysis was performed using SPSS version 26.0 software (IBM SPSS, Armonk, NY, USA), in which $p < 0.05$ was considered statistically significant. All the figures were created with Origin 8.5 software (Origin Lab, Hampton, NH, USA).

## Results and discussion

### Analysis of structural characterization of $EUP_1$, $EUP_2$ and $EUP_3$

#### *Extraction, purification and molecular weight analysis*

Microwave-assisted hot water was used to extract crude polysaccharides from *E. ulmoides* leaves. The extraction rate of crude polysaccharides was 6.5 ± 0.3%. The crude polysaccharides were separated and purified to obtain three components: $EUP_1$, $EUP_2$, and $EUP_3$ (Fig. 1A).

Molecular weight is an important characteristic of polysaccharides, and a key factor affecting antioxidant, antibacterial, immune regulation and other biological activities of polysaccharides [23]. The chromatographic diagram of SEC–MALLS showed that $EUP_1$, $EUP_2$ and $EUP_3$ were all one main peak, indicating that the three components were homogeneous [24]. The average molecular weights ($M_w$) of $EUP_1$, $EUP_2$ and $EUP_3$ were $1.51\times10^5$ Da, $3.05\times10^4$ Da and $1.17\times10^5$ Da, respectively. Meanwhile, the $M_w/M_n$ coefficients of $EUP_1$, $EUP_2$ and $EUP_3$ were 1.24, 1.40 and 1.41, respectively, indicating that the three components were evenly distributed and concentrated (Fig. 1B).

#### *Monosaccharide composition analysis*

GC–MS chromatograms showed that $EUP_1$, $EUP_2$ and $EUP_3$ were mainly composed of *Rha*, *Ara*, *Man*, *Glu* and *Gal*, among which the content of *Gal* and *Ara* was the highest. A small amount of *Xyl* (2.6 mol%) was also detected in $EUP_2$. However, the molar percentage of monosaccharide was different among the three components. The highest content of *Rha* and *Glu* was $EUP_3$, and the highest content of *Ara* and *Gal* was $EUP_1$. Meanwhile, the highest content of *Man* was $EUP_2$. The monosaccharide compositions of $EUP_1$, $EUP_2$ and $EUP_3$ were significantly different ($p < 0.05$) (Table 1).

#### *FT-IR analysis*

The FT-IR spectrum showed that $EUP_1$, $EUP_2$ and $EUP_3$ had similar characteristic peaks. There was a strong and wide characteristic absorption peak at 3400 $cm^{-1}$, which was caused by O–H stretching vibration of the polysaccharides hydroxyl and hydrogen bond. The weak absorption peak at 2930 $cm^{-1}$ was C–H antisymmetric stretching vibration of $CH_3$ and $CH_2$ groups [25], and

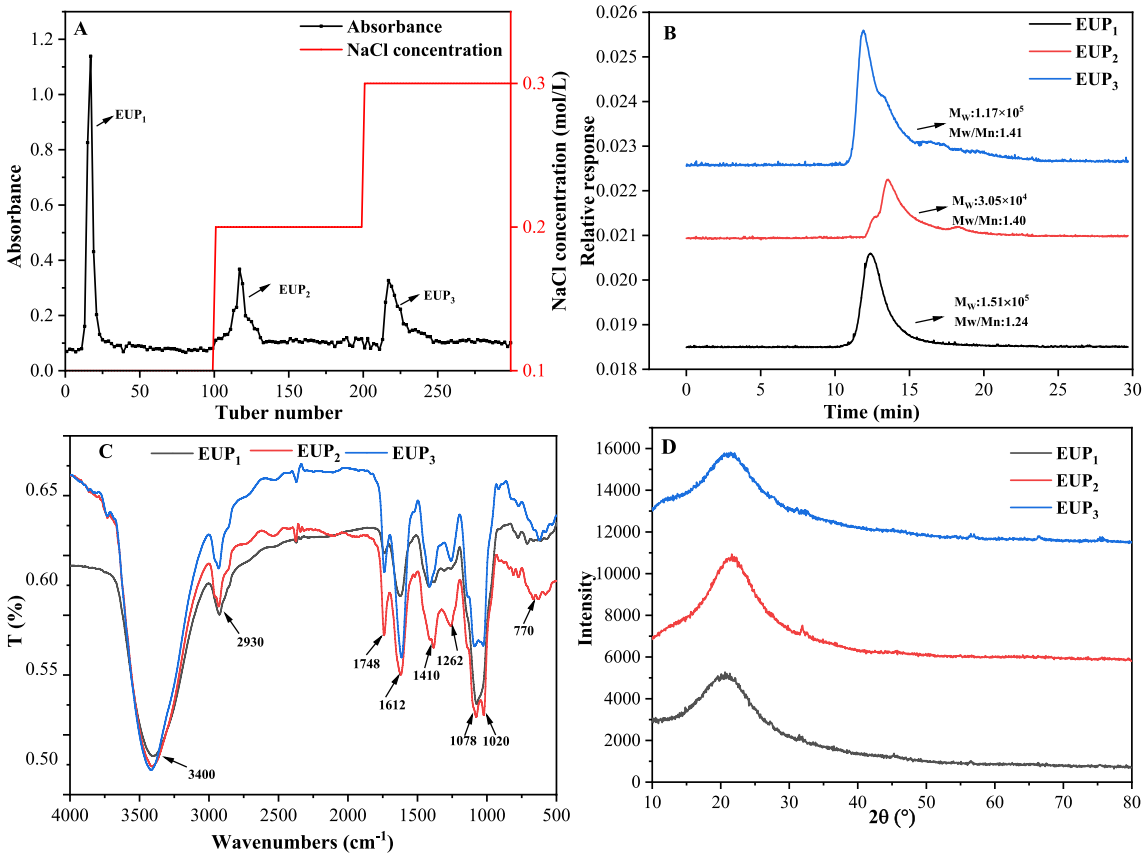


**Fig. 1** Elution profiles, molecular weight, FT-IR spectra and X-ray diffraction analysis of $EUP_1$, $EUP_2$ and $EUP_3$. **A** Elution profiles. **B** Molecular weight map. **C** FT-IR spectra. **D** X-ray diffraction

**Table 1** Monosaccharide composition of $EUP_1$, $EUP_2$ and $EUP_3$

| Samples | Monosaccharide (mol %) | | | | | |
|---|---|---|---|---|---|---|
| | *Rha* | *Ara* | *Xyl* | *Man* | *Glu* | *Gal* |
| $EUP_1$ | $3.6 \pm 0.2^c$ | $29.6 \pm 0.7^a$ | – | $4.5 \pm 0.2^c$ | $14.0 \pm 0.3^b$ | $48.0 \pm 0.6^a$ |
| $EUP_2$ | $8.0 \pm 0.1^b$ | $26.0 \pm 0.4^b$ | $2.6 \pm 0.2$ | $9.0 \pm 0.1^a$ | $13.4 \pm 0.6^b$ | $41.0 \pm 1.0^b$ |
| $EUP_3$ | $18.6 \pm 0.1^a$ | $23.5 \pm 1.1^c$ | – | $5.2 \pm 0.5^b$ | $16.0 \pm 0.7^a$ | $36.7 \pm 1.0^c$ |

Values are the mean of three determinations ± SE (standard error). Different letters indicate significant difference between different components by Tukey's test ($p < 0.05$)

the peak at 1748 $cm^{-1}$ was the absorption peak produced by the tensile vibration of lipid carbonyl C=O. Additionally, there were C=O tensile vibration of the carboxyl group at 1612 $cm^{-1}$ and C–H/O–H bending vibration at 1410 $cm^{-1}$, which indicated aldehyde acids existed, and $EUP_1$, $EUP_2$ and $EUP_3$ were acidic polysaccharides [26]. There was an absorption peak at 1262 $cm^{-1}$, indicating that the polysaccharides contained acetyl groups, and the absorption peaks at 1078 $cm^{-1}$ and 1020 $cm^{-1}$ indicated that the polysaccharides had pyranoid sugar rings [27]. Moreover, a small peak at 770 $cm^{-1}$ showed the β configuration of the sugar unit. Therefore, the structures of $EUP_1$, $EUP_2$ and $EUP_3$ were inferred to be a pyranose structure with β configuration (Fig. 1C).

#### *Crystal structure analysis*

XRD is an important method to quickly study the microstructure of crystals or some amorphous materials. The diffraction peaks of crystalline materials are narrow and sharp, while those of amorphous materials are scattered and wide [28]. According to the XRD diffraction diagram, $EUP_1$, $EUP_2$ and $EUP_3$ only showed a single bread-like peak at $2\theta = 20°$, which showed that the crystallization of three components was amorphous structure (Fig. 1D).

#### *NMR analysis*

NMR spectroscopy is the most powerful technique for the structural analysis of complex polysaccharides, which can simplify the structural analysis of carbohydrates. In the $^1H$ NMR spectra of the three components, most of the signals appeared in the range of $\delta_H$3.4–5.2 ppm, and there was no signal at $\delta_H$5.4 ppm, indicating that $EUP_1$, $EUP_2$, and $EUP_3$ were pyrano polysaccharides (Fig. 2). The signal at $\delta_H$5.1–5.2 ppm indicated α configuration in monosaccharide residues, and the strong peak signal near $\delta_C$103–109 ppm and $\delta_H$4.3 ppm showed β configuration in monosaccharide residues [29]. The results were consistent with that of the FTIR spectrum analysis. Moreover, the $\delta_H$1.2 ppm and $\delta_H$1.1 ppm signals were derived from the methoxyl groups of O-2 and O-2, 4-linked *Rha*, respectively. The signal at $\delta_H$1.9–2.3 ppm was assigned to the acetyl group, and $\delta_H$3.42–3.86 ppm was the chemical shift of protons on polysaccharides C2–C6 [30]. A massive signal at $\delta_H$3.67 ppm was from the methoxy group bound to the carboxyl group of *Gal* [31]. The proton signal of *Ara* residues was observed at $\delta_H$5.0 ppm, $\delta_H$4.5 ppm, $\delta_H$4.03 ppm, $\delta_H$4.1 ppm, and $\delta_H$3.8 ppm. The enhanced degree shift at $\delta_H$4.6 ppm can be attributed to the solvent $D_2O$.

In the $^{13}C$ NMR spectrum, signals near $\delta_C$ 16.6 ppm were confirmed to be associated with $CH_3$ of *Rha*. The dense distribution of carbon signal between $\delta_C$ 60.0–75.1 ppm was related to the absorption signal of C2–C5 in monosaccharides, while the resonance signal region of C6 was located at $\delta_C$ 60–65.1 ppm [32]. Meanwhile, the $\delta_C$ 109.3 ppm and $\delta_C$ 107.4 ppm signals were attributed to different C-1 bonds of *Rha*, and the $\delta_C$100 ppm signal was attributed to different C-1 bonds of *Gal* [33].

#### *Apparent morphology analysis*

The surface morphology of polysaccharides can be effectively observed by FE-SEM (Fig. 3). It was found that the three components had different surface structures. Among them, $EUP_1$ resembled a honeycomb with loose and porous surface morphology, while $EUP_2$ presented a rod-like shape with rough and branching surface, and $EUP_3$ was mainly a flake structure with smooth surface. The differences in surface morphology of three components indicated that the strengths of aggregation and bonding were different (Fig. 3). 3.2 Analysis of physicochemical property of $EUP_1$, $EUP_2$ and $EUP_3$.

#### *Zeta potential and particle size analysis*

Zeta potential analysis showed that $EUP_1$ potential was − 11.47 mV, while $EUP_2$ potential and $EUP_3$ potential were − 14.5 mV and − 16.63 mV, respectively. Therefore, the three elution components of *E. ulmoides* polysaccharides were acidic polysaccharides, and the absolute values of ζ potential of three components increased with the increase of eluent concentration, which was consistent with the elution mechanism of ion chromatography [34]. The average particle size of $EUP_1$ (964.97 nm) was

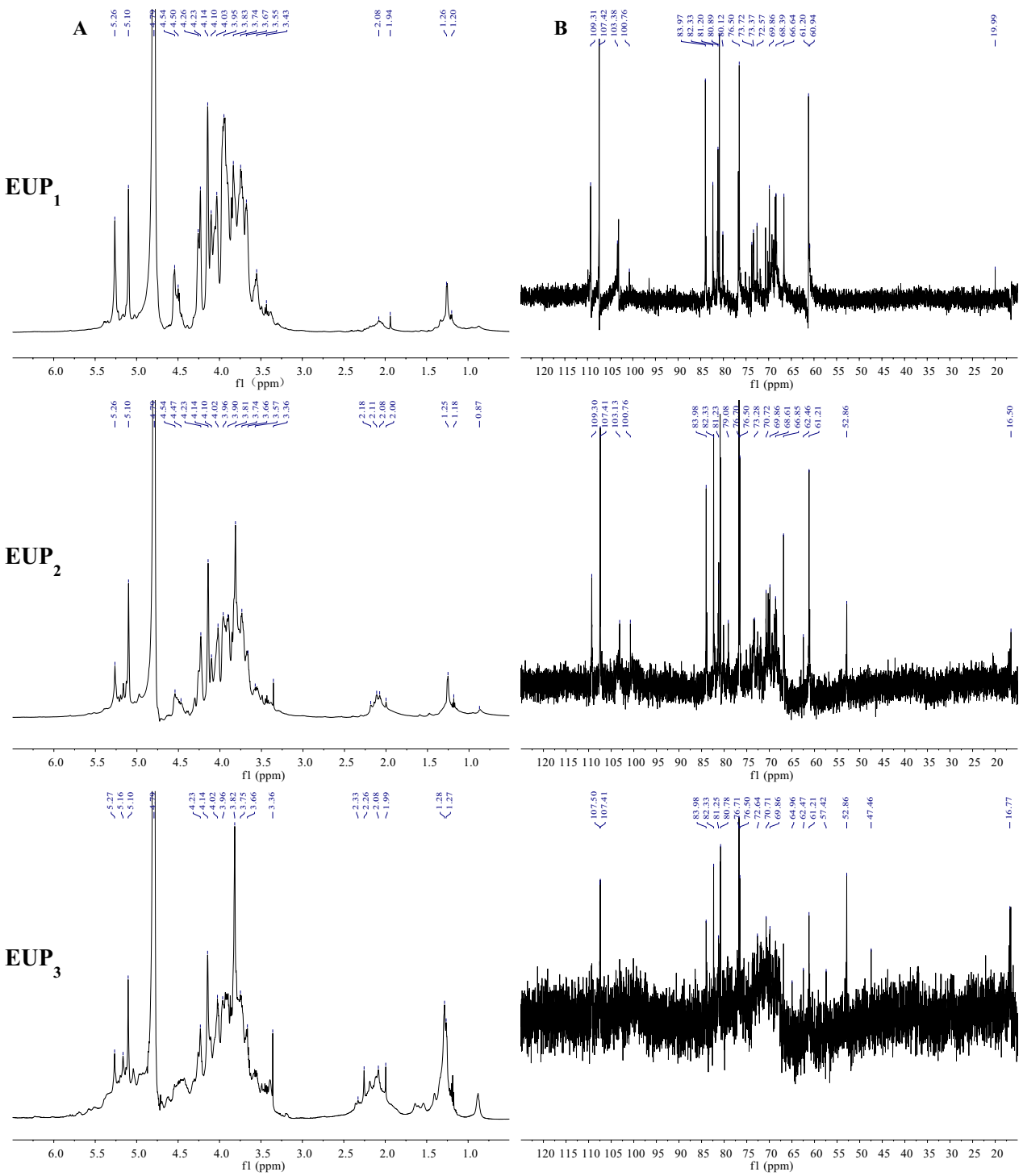


**Fig. 2** NMR spectra of $EUP_1$, $EUP_2$ and $EUP_3$. **A** $^1H$ spectrum. **B** $^{13}C$ spectrum

the largest, followed by $EUP_2$ (816.97 nm) and $EUP_3$ (284.93 nm). The average particle size of the three components decreased with the increase of eluent concentration, which may be because the larger the absolute value of ζ potential, the stronger the electrostatic repulsion between particles and the formation of a more dispersed system between particles [35]. The greater the absolute

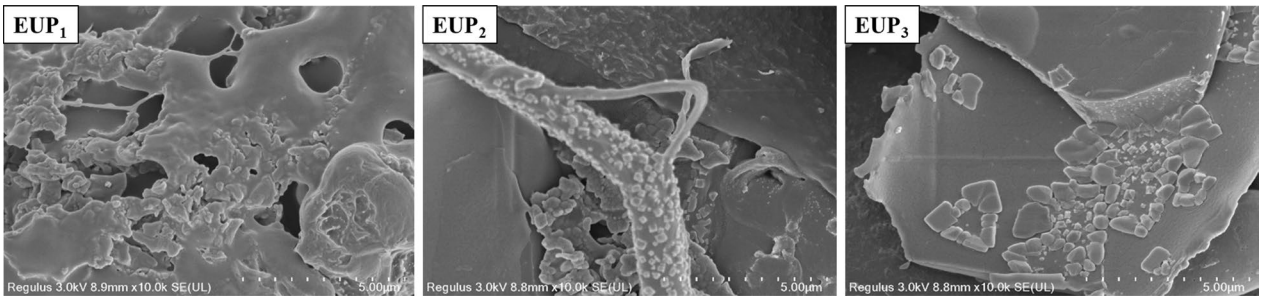


**Fig. 3** Scanning electron micrographs of $EUP_1$, $EUP_2$ and $EUP_3$ (10.0K×)

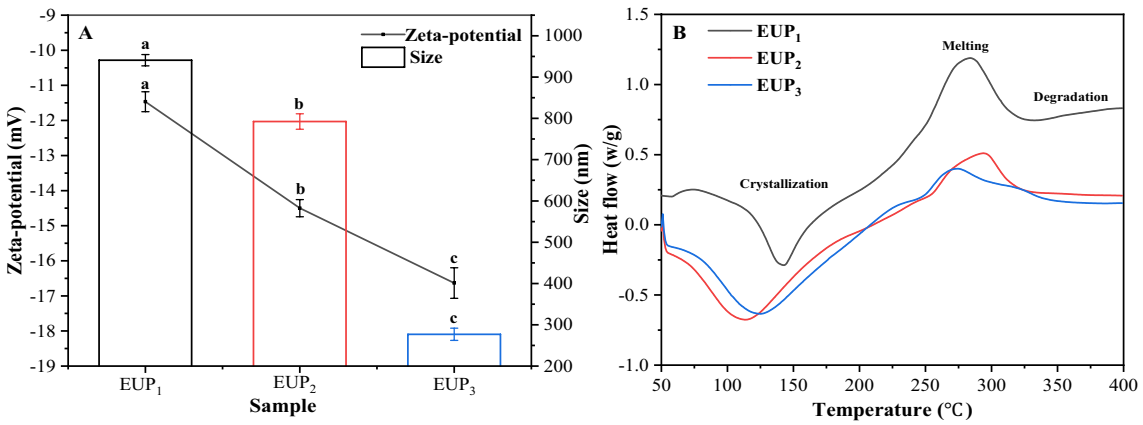


**Fig. 4** Average particle size, potential diagram and DSC curve of $EUP_1$, $EUP_2$ and $EUP_3$. **A** Average particle size and potential diagram. **B** DSC curve. The standard error of the mean is denoted by a capped bar at the top of each column. Different letters indicate significant difference between different components by Tukey's test ($p < 0.05$)

value of ζ potential, the smaller the mean particle size (Fig. 4A).

### *Thermal stability analysis*

Thermal stability is an important feature of various biomolecules for biological applications. DSC curves showed that the endothermic reactions of $EUP_1$, $EUP_2$ and $EUP_3$ occurred within 100–150 ℃, among which the crystallization temperatures of $EUP_2$ and $EUP_3$ were about 120 ℃, and that of $EUP_1$ was 142 ℃ (Fig. 4B). The melting of polysaccharides occurred with an exothermic reaction between 270 and 300 °C. Therefore, the thermodynamic curve showed that these three components have certain thermal stability in the temperature range below 270 ℃. Additionally, the reaction enthalpy of $EUP_1$ was 103.6 J/g, which was much higher than that of $EUP_2$ (66.78 J/g) and $EUP_3$ (52.94 J/g). $EUP_1$ had the highest thermal stability, while $EUP_2$ and $EUP_3$ had similar thermal stability. The difference in thermal stability of three components may be caused by the different monosaccharide composition and molecular weight [36].

### Analysis of antioxidant activity of $EUP_1$, $EUP_2$ and $EUP_3$

Free radicals are naturally generated in human metabolism and can easily attack protein, DNA, lipids and other biological macromolecules to induce oxidative stress. Studies have shown that they are related to tumors, cancers, cardiovascular diseases and other diseases [37]. ESR method is the most direct method to detect free radicals. It is based on the principle that unpaired electrons absorb electromagnetic radiation in the DC magnetic field and transition from a low energy level to a high energy level, which can avoid the influence of sample color [38].

### *DPPH radical scavenging activity analysis*

The DPPH free radical is a relatively stable free radical at room temperature and has been widely used to evaluate the antioxidant capacity of polysaccharides. In the range of 0.04–0.24 mg/mL, all three components had strong

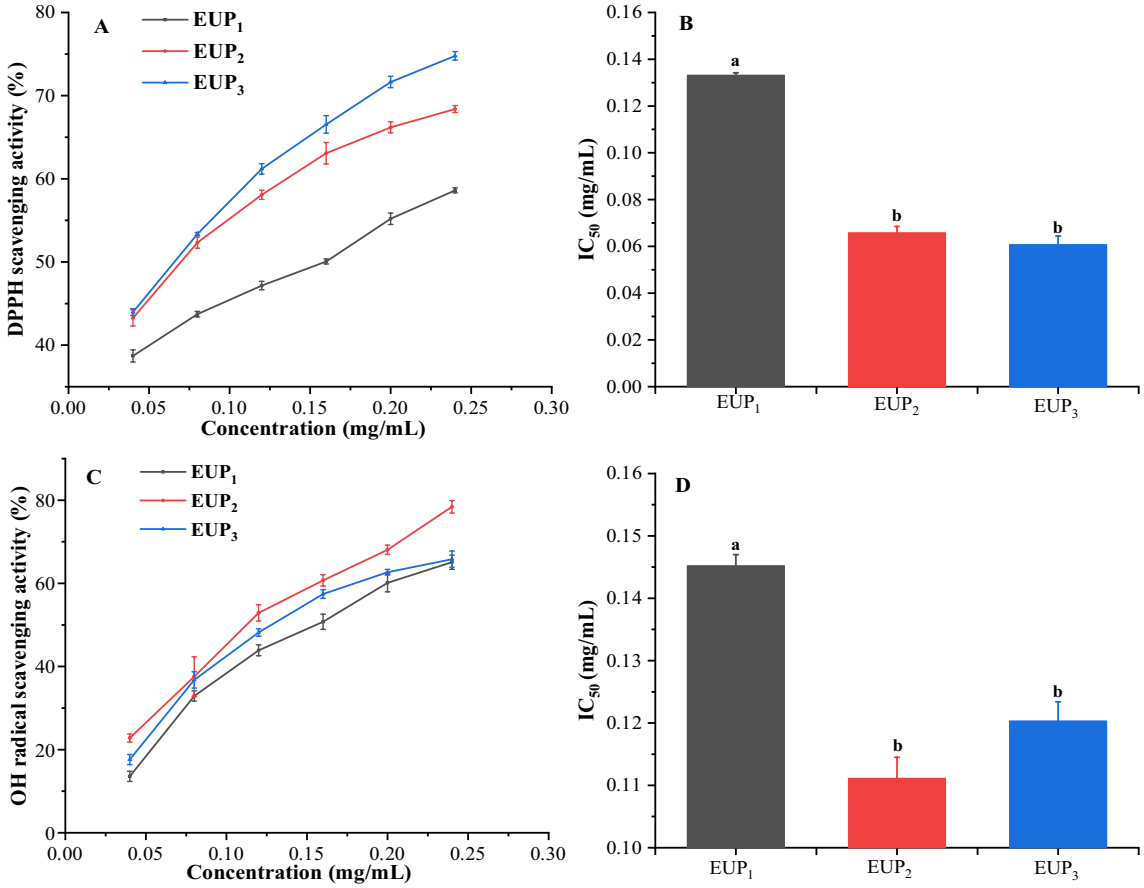


**Fig. 5** Antioxidant activity of $EUP_1$, $EUP_2$ and $EUP_3$. **A** DPPH radical scavenging activity. **B** $IC_{50}$ of DPPH radical scavenging activity. **C** OH radical scavenging activity. **D** $IC_{50}$ of OH radical scavenging activity. The standard error of the mean is denoted by a capped bar at the top of each column. Different letters indicate significant difference between different components by Tukey's test ($p < 0.05$)

DPPH free radical scavenging ability, and the free radical scavenging ability increased with the increase of concentration, showing a significant dose relationship. When the concentration was 0.24 mg/mL, the DPPH radical scavenging ability of $EUP_1$, $EUP_2$ and $EUP_3$ reached 58.6%, 68.4% and 74.5%, respectively (Fig. 5A). Meanwhile, the $IC_{50}$ values of $EUP_1$, $EUP_2$ and $EUP_3$ scavenging DPPH free radical were 0.13, 0.07 and 0.06, respectively (Fig. 5B). $EUP_2$ and $EUP_3$ had no significant difference in the DPPH scavenging activity, but both of them were superior to $EUP_1$ ($p < 0.05$).

### *OH radical scavenging activity analysis*

In the range of 0.04–0.24 mg/mL, the scavenging ability of the three components to OH radicals increased with the increase in concentration, and the $IC_{50}$ of $EUP_1$, $EUP_2$ and $EUP_3$ were 0.15 mg/mL, 0.11 mg/mL and 0.12 mg/mL, respectively (Fig. 5C and D). Similar to the DPPH radical scavenging activity, there was no significant difference in OH scavenging ability between $EUP_2$ and $EUP_3$, but both of them were superior to $EUP_1$ ($p < 0.05$).

The differences in the antioxidant capacity of $EUP_1$, $EUP_2$ and $EUP_3$ may be caused by different molecular weight, monosaccharide composition, substituent position and branching degree. $EUP_1$ had the highest molecular weight, but the scavenging capacity of DPPH and OH radical was lower than that of $EUP_2$ and $EUP_3$ with smaller molecular weight. This result indicated that polysaccharides with smaller molecular weight had higher antioxidant capacity within a certain range, which was consistent with the results of Long et al. [39]. In addition, the study by Lo et al. [40] showed that the free radical scavenging ability of polysaccharides depended on their monosaccharide composition, and *Rha* was the most important factor related to the free radical scavenging ability of polysaccharides. In this research, the mole ratio of *Rha* in $EUP_1$ was 3.66 mol%, which was much lower than that in $EUP_2$ (7.92 mol%) and $EUP_3$ (18.67 mol%).

## Conclusion

In this research, crude polysaccharides from *E. ulmoides* leaves were extracted by microwave assisted hot water with an extraction rate of 6.5 ± 0.3%, and three components $EUP_1$, $EUP_2$ and $EUP_3$ were purified and obtained through anion exchange column. The structure, physicochemical property and antioxidant activity of $EUP_1$, $EUP_2$ and $EUP_3$ were studied by SEC–MALLS, GC–MS, FT-IR, XRD, NMR, FE-SEM, DSC and ESR methods. The results showed that the three components all had typical polysaccharides absorption peaks, which may be polysaccharides with β configuration of pyranose structure, and amorphous structure of acid polysaccharides with good thermal stability below 270 ℃. However, the molecular weight, monosaccharide composition and apparent morphology of the three components were different, leading to the superior scavenging ability of DPPH and OH radicals of $EUP_2$ and $EUP_3$. The results will provide a reference for developing *E. ulmoides* leaves as well as a basis for developing a new antioxidant.

#### Author contributions

ML, YW and LW: methodology, writing—review and editing, project administration. RW and QD: data curation, writing—original draft.

#### Funding

This work was supported by the National key research and development project (2017YFD060130205).

#### Data availability

All data generated or analyzed during this study are included in this published article.

## Declarations

#### Ethics approval and consent to participate

Not applicable.

#### Competing interests

The authors declare no financial or other competing interests in this work.

#### Author details

[1]College of Food and Bioengineering, Zhengzhou University of Light Industry, Zhengzhou 450002, China. [2]State Key Laboratory of Tree Genetics and Breeding, Key Laboratory of Non-Timber Forest Germplasm Enhancement & Utilization of State Administration of Forestry and Grassland, Research Institute of Non-Timber Forestry, Chinese Academy of Forestry, Zhengzhou 450003, China.

Received: 22 September 2023 Accepted: 18 October 2023
Published online: 31 October 2023

#### References

1. Huang L, Lyu Q, Zheng W, Yang Q, Cao G. Traditional application and modern pharmacological research of *Eucommia ulmoides* Oliv. Chin Med. 2021;16:73. https://doi.org/10.1186/s13020-021-00482-7.
2. He X, Wang J, Li M, Hao D, Yang Y, Zhang C, He R, Tao R. *Eucommia ulmoides* Oliv.: ethnopharmacology, phytochemistry and pharmacology of an important traditional Chinese medicine. J Ethnopharmacol. 2014;151:78–92. https://doi.org/10.1016/j.jep.2013.11.023.
3. Xing YF, He D, Wang Y, Zeng W, Zhang C, Lu Y, Su N, Kong YH, Xing XH. Chemical constituents, biological functions and pharmacological effects for comprehensive utilization of *Eucommia ulmoides* Oliver. Food Sci Hum Wellness. 2019;8:177–88. https://doi.org/10.1016/j.fshw.2019.03.013.
4. Xiaolong J, Jianhang G, Tengzheng C, Tingting Z, Yanqi L, Yizhe Y. Review on mechanisms and structure-activity relationship of hypoglycemic effects of polysaccharides from natural resources. Food Sci Hum Wellness. 2023;12(6):1969–80. https://doi.org/10.1016/j.fshw.2023.03.017.
5. Jin M, Huang Q, Zhao K, Shang P. Biological activities and potential health benefit effects of polysaccharides isolated from *Lycium barbarum* L. Int J Biol Macromol. 2013;54:16–23. https://doi.org/10.1016/j.ijbiomac.2012.11.023.
6. Tang Y, Zhu ZY, Liu Y, Sun H, Song QY, Zhang Y. The chemical structure and anti-aging bioactivity of an acid polysaccharide obtained from rose buds. Food Funct. 2018;9:2300–12. https://doi.org/10.1039/C8FO00206A.
7. Ji X, Cheng Y, Tian J, Zhang S, Jing Y, Shi M. Structural characterization of polysaccharide from jujube (*Ziziphus jujuba* Mill.) fruit. Chem Biol Technol Agric. 2021;8:54. https://doi.org/10.1186/s40538-021-00255-2.
8. Ji X, Guo J, Ding D, Gao J, Hao L, Guo X, Liu Y. Structural characterization and antioxidant activity of a novel high-molecular-weight polysaccharide from *Ziziphus Jujuba* cv. *Muzao*. J Food Meas Charact. 2022;16:2191–200. https://doi.org/10.1007/s11694-022-01288-3.
9. Xu J, Hou H, Hu J, Liu B. Optimized microwave extraction, characterization and antioxidant capacity of biological polysaccharides from *Eucommia ulmoides* Oliver leaf. Sci Rep. 2018;8:6561. https://doi.org/10.1038/s41598-018-24957-0.
10. Liu M, Lu W, Ku K, Zhangm L, Lei L, Zong W. Ultrasonic-assisted extraction and antioxidant activity of polysaccharides from *Eucommia ulmoides* leaf. Pak J Pharm Sci. 2020;33:581–8. https://doi.org/10.36721/PJPS.2020.33.2.REG.581-588.1.
11. Sun Y, Huang K, Mo L, Ahmad A, Wang D, Rong Z, Peng H, Cai H, Liu G. *Eucommia ulmoides* polysaccharides attenuate rabbit osteoarthritis by regulating the function of macrophages. Front Pharmacol. 2021;12:730557. https://doi.org/10.3389/fphar.2021.730557.
12. Deng Y, Ma F, Ruiz-Ortega LI, Peng Y, Tian Y, He W, Tang B. Fabrication of strontium *Eucommia ulmoides* polysaccharides and in vitro evaluation of their osteoimmunomodulatory property. Int J Biol Macromol. 2019;140:727–35. https://doi.org/10.1016/j.ijbiomac.2019.08.145.
13. Gao W, Feng Z, Zhang S, Wu B, Geng X, Fan G, Duan Y, Li K, Liu K, Peng C. Anti-inflammatory and antioxidant effect of *Eucommia ulmoides* polysaccharide in hepatic Ischemia-reperfusion injury by regulating ROS and the TLR-4-NF-κ B pathway. BioMed Res Int. 2020. https://doi.org/10.1155/2020/1860637.
14. Rostami H, Gharibzahedi SMT. Microwave-assisted extraction of jujube polysaccharide: optimization, purification and functional characterization. Carbohyd Polym. 2016;143:100–7. https://doi.org/10.1016/j.carbpol.2016.01.075.
15. Sun H, Li C, Ni Y, Yao L, Jiang H, Ren X, Fu Y, Zhao C. Ultrasonic/microwave-assisted extraction of polysaccharides from *Camptotheca acuminata* fruits and its antitumor activity. Carbohyd Polym. 2019;12:730557. https://doi.org/10.1016/j.carbpol.2018.11.010.
16. Chen P, You Q, Li X, Chang Q, Zhang Y, Zheng B, Hu X, Zeng H. Polysaccharide fractions from *Fortunella margarita* affect proliferation of *Bifidobacterium adolescentis* ATCC 15703 and undergo structural changes following fermentation. Int J Biol Macromol. 2019;123:1070–8. https://doi.org/10.1016/j.ijbiomac.2018.11.163.
17. Sheng Z, Wen L, Yang B. Structure identification of a polysaccharide in mushroom Lingzhi spore and its immunomodulatory activity. Carbohyd Polym. 2022;278:118939. https://doi.org/10.1016/j.carbpol.2021.118939.
18. Wang F, Ye S, Ding Y, Ma Z, Zhao Q, Zang M, Li Y. Research on structure and antioxidant activity of polysaccharides from *Ginkgo biloba* leaves. J Mol Struct. 2022;1252:132185. https://doi.org/10.1016/j.molstruc.2021.132185.
19. Kazemi M, Khodaiyan F, Labbafi M, Saeid Hosseini S, Hojjati M. Pistachio green hull pectin: optimization of microwave-assisted extraction and evaluation of its physicochemical, structural and functional properties. Food Chem. 2019;271:663–72. https://doi.org/10.1016/j.foodchem.2018.07.212.
20. Ren Y, Liu S. Effects of separation and purification on structural characteristics of polysaccharide from quinoa (*Chenopodium quinoa* willd).

Biochem Bioph Res Co. 2020;522:286–91. https://doi.org/10.1016/j.bbrc.2019.10.030.
21. Peng X, Xiong YL, Kong B. Antioxidant activity of peptide fractions from whey protein hydrolysates as measured by electron spin resonance. Food Chem. 2009;113:196–201. https://doi.org/10.1016/j.foodchem.2008.07.068.
22. Hu T, Liu D, Chen Y, Wu J, Wang S. Antioxidant activity of sulfated polysaccharide fractions extracted from *Undaria pinnitafida* in vitro. Int J Biol Macromol. 2010;46:193–8. https://doi.org/10.1016/j.ijbiomac.2009.12.004.
23. Yuan J, Chen S, Wang L, Xu T, Shi X, Jing Y, Zhang H, Huang Y, Xu Y, Li D, Chen X, Chen J, Xiong Q. Preparation of purified fractions for polysaccharides from *Monetaria moneta* Linnaeus and comparison their characteristics and antioxidant activities. Int J Biol Macromol. 2018;108:342–9. https://doi.org/10.1016/j.ijbiomac.2017.12.023.
24. Yang Y, Chang Y, Wu Y, Liu H, Liu Q, Kang Z, Wu M, Yin H, Duan J. A homogeneous polysaccharide from *Lycium barbarum*: structural characterizations, anti-obesity effects and impacts on gut microbiota. Int J Biol Macromol. 2021;183:2074–87. https://doi.org/10.1016/j.ijbiomac.2021.05.209.
25. Zhao W, Zhang W, Liu L, Cheng Y, Guo Y, Yao W, Qian H. Fractionation, characterization and anti-fatigue activity of polysaccharides from *Brassica rapa* L. Process Biochem. 2021;106:163–75. https://doi.org/10.1016/j.procbio.2021.04.016.
26. Yuan Q, He Y, Xiang PY, Huang YJ, Cao ZW, Shen SW, Zhao L, Zhang Q, Qin W, Wu DT. Influences of different drying methods on the structural characteristics and multiple bioactivities of polysaccharides from okra (*Abelmoschus esculentus*). Int J Biol Macromol. 2020;147:1053–63. https://doi.org/10.1016/j.ijbiomac.2019.10.073.
27. Hashemifesharaki R, Xanthakis E, Altintas Z, Guo Y, Gharibzahedi SMT. Microwave-assisted extraction of polysaccharides from the marshmallow roots: optimization, purification, structure, and bioactivity. Carbohyd Polym. 2020;240:116301. https://doi.org/10.1016/j.carbpol.2020.116301.
28. Patel MK, Tanna B, Mishra A, Jha B. Physicochemical characterization, antioxidant and anti-proliferative activities of a polysaccharide extracted from psyllium (*P. ovata*) leaves. Int J Biol Macromol. 2018;118:976–87. https://doi.org/10.1016/j.ijbiomac.2018.06.139.
29. Yao HYY, Wang JQ, Yin JY, Nie SP, Xie MY. A review of NMR analysis in polysaccharide structure and conformation: progress, challenge and perspective. Food Res Int. 2021;143:110290. https://doi.org/10.1016/j.foodres.2021.110290.
30. Wang L, Liu F, Wang A, Yu Z, Xu Y, Yang Y. Purification, characterization and bioactivity determination of a novel polysaccharide from pumpkin (*Cucurbita moschata*) seeds. Food Hydrocoll. 2017;66:357–64. https://doi.org/10.1016/j.foodhyd.2016.12.003.
31. Wang W, Ma X, Jiang P, Hu L, Zhi Z, Chen J, Ding T, Ye X, Liu D. Characterization of pectin from grapefruit peel: a comparison of ultrasound-assisted and conventional heating extractions. Food Hydrocoll. 2016;61:730–9. https://doi.org/10.1016/j.foodhyd.2016.06.019.
32. Liang X, Gao Y, Pan Y, Zou Y, He M, He C, Li L, Yin Z, Lv C. Purification, chemical characterization and antioxidant activities of polysaccharides isolated from *Mycena dendrobii*. Carbohyd Polym. 2019;203:45–51. https://doi.org/10.1016/j.carbpol.2018.09.046.
33. Huang C, Yao R, Zhu Z, Pang D, Cao X, Feng B, Paulsen BS, Li L, Yin Z, Chen X, Jia R, Song X, Ye G, Luo Q, Chen Z, Zou Y. A pectic polysaccharide from water decoction of Xinjiang *Lycium barbarum* fruit protects against intestinal endoplasmic reticulum stress. Int J Biol Macromol. 2019;130:508–14. https://doi.org/10.1016/j.ijbiomac.2019.02.157.
34. Dong X, Zhu CP, Huang GQ, Xiao JX. Fractionation and structural characterization of polysaccharides derived from red grape pomace. Process Biochem. 2021;109:37–45. https://doi.org/10.1016/j.procbio.2021.06.022.
35. Ghasemi S, Jafari SM, Assadpour E, Khomeiri M. Nanoencapsulation of d-limonene within nanocarriers produced by pectin-whey protein complexes. Food Hydrocoll. 2018;77:152–62. https://doi.org/10.1016/j.foodhyd.2017.09.030.
36. Rozi P, Abuduwaili A, Mutailifu P, Gao Y, Rakhmanberdieva R, Aisa HA, Yili A. Sequential extraction, characterization and antioxidant activity of polysaccharides from *Fritillaria pallidiflora* Schrenk. Int J Biol Macromol. 2019;131:97–106. https://doi.org/10.1016/j.ijbiomac.2019.03.029.
37. Zang S, Tian S, Jiang J, Han D, Yu X, Wang K, Li D, Lu D, Yu A, Zhang Z. Determination of antioxidant capacity of diverse fruits by electron spin resonance (ESR) and UV–vis spectrometries. Food Chem. 2017;221:1221–5. https://doi.org/10.1016/j.foodchem.2016.11.036.
38. Bartoszek M, Polak J. A comparison of antioxidative capacities of fruit juices, drinks and nectars, as determined by EPR and UV–vis spectroscopies. Spectrochim Acta A. 2016;153:546–9. https://doi.org/10.1016/j.saa.2015.09.022.
39. Long X, Hu X, Liu S, Pan C, Chen S, Li L, Qi B, Yang X. Insights on preparation, structure and activities of *Gracilaria lemaneiformis* polysaccharide. Food Chem. 2021;12:100153. https://doi.org/10.1016/j.fochx.2021.100153.
40. Lo TCT, Chang CA, Chiu KH, Tsay PK, Jen JF. Correlation evaluation of antioxidant properties on the monosaccharide components and glycosyl linkages of polysaccharide with different measuring methods. Carbohyd Polym. 2011;86:320–7. https://doi.org/10.1016/j.carbpol.2011.04.056.

## Publisher's Note